JACS
JOURNAL OF THE AMERICAN CHEMICAL SOCIETY
Communication
pubs.acs.org/JACS

The Power of Packing: Metallization of an Organic Semiconductor

Aaron Mailman,[†] Alicea A. Leitch,[†] Wenjun Yong,[‡] Eden Steven,[⊥] Stephen M. Winter,[†] Robert C. M. Claridge,[†] Abdeljalil Assoud,[†] John S. Tse,[§] Serge Desgreniers,[▽] Richard A. Secco,[‡] and Richard T. Oakley*[,†]

[†]Department of Chemistry, University of Waterloo, Waterloo, Ontario N2L 3G1, Canada
[‡]Department of Earth Sciences, University of Western Ontario, London, Ontario N6A 5B7, Canada
[⊥]Department of Physics, Florida State University, Tallahassee, Florida 32310, United States
[§]Department of Physics, University of Saskatchewan, Saskatoon, Saskatchewan S7N 5E2, Canada
[▽]Department of Physics, University of Ottawa, Ottawa, Ontario K1N 6N5, Canada

Supporting Information

ABSTRACT: Benzoquino-bis-1,2,3-dithiazole **5** is a closed shell, antiaromatic 16π-electron zwitterion with a small HOMO−LUMO gap. Its crystal structure consists of planar ribbon-like molecular arrays packed into offset layers to generate a "brick-wall" motif with strong 2D interlayer electronic interactions. The spread of the valence and conduction bands, coupled with the narrow HOMO−LUMO gap, affords a small band gap semiconductor with σ_{RT} = 1 × 10^{-3} S cm^{-1} and E_{act} = 0.14 eV for transport within the brick-wall arrays. Closure of the band gap to form an all-organic molecular metal with σ_{RT} > 10^{1} S cm^{-1} can be achieved by the application of pressure to 8 GPa.

In the absence of an electric field, chemical doping, or photoexcitation most closed shell organic molecular solids are insulators.[1] The HOMO−LUMO gaps are too large, and intermolecular interactions too small to generate spreading of the valence and/or conduction bands and allow closure of the band gap E_g. A variety of strategies to reduce the HOMO−LUMO separation and improve charge transport have been considered.[2] Notable targets have included formally antiaromatic (4nπ) systems such as quinonemonoimines **1**, hexaazaanthracenes **2** and bisdithiazoles **3** (Chart 1) in which a charge-separated zwitterionic singlet state competes with a triplet or singlet biradical.[3−5] These and related materials have been explored extensively, as the HOMO−LUMO gap, and consequent singlet/triplet splitting ΔE_{ST}, can be fine-tuned by variations in substituents and heteroatoms. However, reduction of the band gap to the point where charge carriers can be easily generated by thermal excitation has remained a challenge.[6]

Chart 1

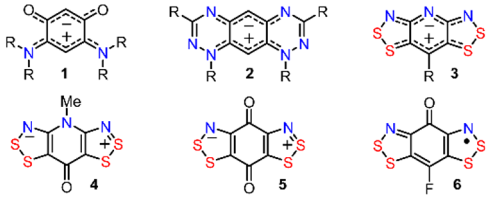

Further reduction in the HOMO−LUMO gap can be made by incorporating a pyridone or benzoquinone bridge, as in the 16π-electron bisdithiazoles **4** and **5**. The former is known to possess a very small HOMO−LUMO gap with ΔE_{ST} near 0.15 eV,[7] but its crystal structure allows for very little band spreading, and it shows no measurable conductivity. By contrast, the quinone-bridged zwitterion **5**, whose preparation and transport properties we describe here, possesses a crystal structure with the much sought after "brick-wall" packing pattern recognized as effective for the development of strong 2D electronic interactions in organic semiconductor devices.[8] As it happens, the zwitterion is isostructural with the 17π-electron oxobenzene-bridged radical **6**,[9] which displays high conductivity at ambient pressure (σ_{RT} ~ 10^{-2} S cm^{-1}), metallizes at 3 GPa and forms a Fermi liquid state at 6 GPa.[10] In the case of **5**, the small HOMO−LUMO gap, combined with the spreading of the valence and conduction bands, affords a small band gap semiconductor with σ_{RT} ~ 10^{-3} S cm^{-1} at ambient pressure. Moreover, the application of physical pressure leads to closure of the band gap and formation of a single component organic metal with σ_{RT} > 10^{1} S cm^{-1} at 8 GPa.

Scheme 1

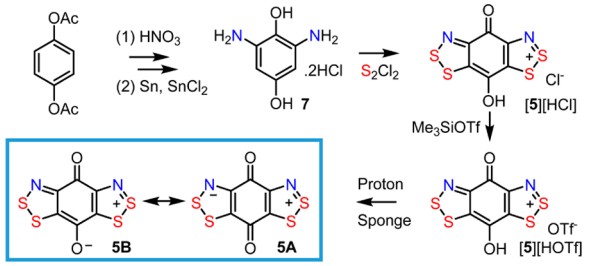

The preparation of **5** (Scheme 1) begins with 2,6-diamino-1,4-dihydroxybenzene **7** (as its bishydrochloride salt), which is prepared by nitration and reduction of commercially available 1,4-diacetoxybenzene.[11] Subsequent condensation of **7** with sulfur monochloride yields the chloride salt of the protonated oxobenzene-bridged bisdithiazolium cation [**5**]H^+, which may be

Received: December 13, 2016
Published: January 31, 2017

© 2017 American Chemical Society

DOI: 10.1021/jacs.6b12814
J. Am. Chem. Soc. 2017, 139, 2180−2183

converted to the more soluble triflate salt by metathesis with trimethylsilyl triflate. Deprotonation of this material with Proton-Sponge yields the zwitterion, which sublimes at 240 °C/10^{-4} Torr to afford air-stable, purple-black crystalline blocks.

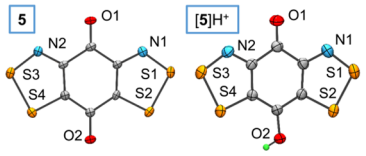

	5	[5]H+
d(S-S)	2.086(4)	2.069(9)
d(S-N)	1.62(2)	1.609(2)
d(N-C)	1.32(1)	1.307(2)
d(C-O1)	1.22(1)	1.211(2)
d(C-O2)	1.25(1)	1.345(2)

Figure 1. ORTEP drawings of **5** and $[\mathbf{5}]H^+$ (in its OTf^- salt) with atom numbering, with selected metrics in Å. For averaged values, numbers in parentheses are the greater of the difference and the standard deviation.

The internal structural metrics of **5**, obtained by single crystal X-ray diffraction (Figure 1), are broadly consistent with the valence bond formulation **5A**. The marked shortening of the C−O2 bond that accompanies deprotonation of the $[\mathbf{5}]H^+$ cation (in the triflate salt) and the resulting similarity in the C−O1 and C−O2 distances suggests little resonance with the internal salt formulation **5B**. The charge density distribution and low molecular dipole moment obtained from DFT calculations at the B3LYP/6-311G(d,p) level are consistent with this interpretation (Figure S11).

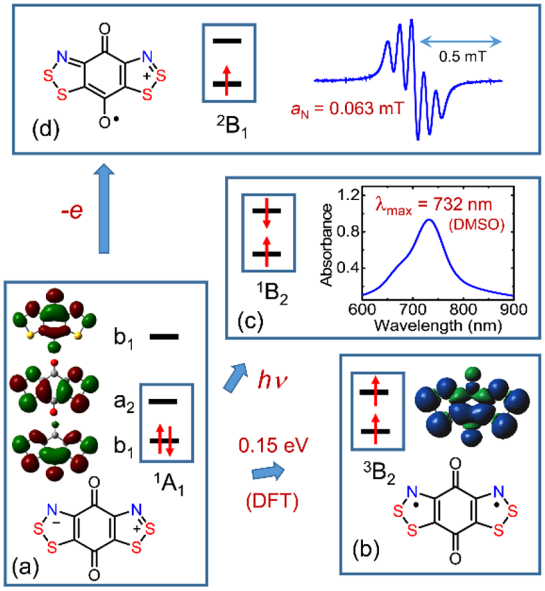

Figure 2. (a) Frontier Kohn−Sham π-orbital manifold (not to scale) of the zwitterionic $^1A_1$ state of **5**, (b) DFT spin distribution of the $^3B_2$ triplet state, (c) $^1B_2$ open shell singlet state of **5** and the $^1A_1$ to $^1B_2$ excitation in the near IR spectrum and (d) EPR spectrum of the $^2B_1$ radical cation $\mathbf{5}^+$ recorded in $SO_2(l)$.

The DFT calculations reveal a frontier π-orbital manifold (Figure 2) for the zwitterionic $^1A_1$ state of **5** consisting of a closely spaced b_1 HOMO and a_2 LUMO, with an additional low-lying b_1 LUMO+1 that is of importance in understanding the solid state electronic features (vide infra). In the $^3B_2$ triplet state, which lies slightly above the zwitterionic singlet, with ΔE_{ST} = 0.15 eV, as found for **4**, spin density is partitioned between the two dithiazole rings. The corresponding open-shell $^1B_2$ singlet lies significantly higher in energy, and photoexcitation to this state gives rise to an intense near IR band at 732 nm (in DMSO), which may be compared with a calculated (TD-DFT) estimate of 837 nm. While **5** is closed shell and EPR silent, the open-shell $^2B_1$ radical cation $[\mathbf{5}]^+$ can be generated in situ by the comproportionation of the doubly oxidized salt $[\mathbf{5}][AlCl_4]_2$ with neutral **5** in liquid SO_2. The resulting EPR spectrum (Figure 2) displays the expected five-line pattern (g = 2.01125), but with a substantially smaller a_N value (0.063 mT) than typically seen in radicals like **6**, an observation suggestive of a semiquinone radical cation formulation.[12] In the case of $[\mathbf{5}]^+$, spin density (Figure S1) is localized on the basal oxygen; the calculated a_N values are consistent with those observed experimentally.

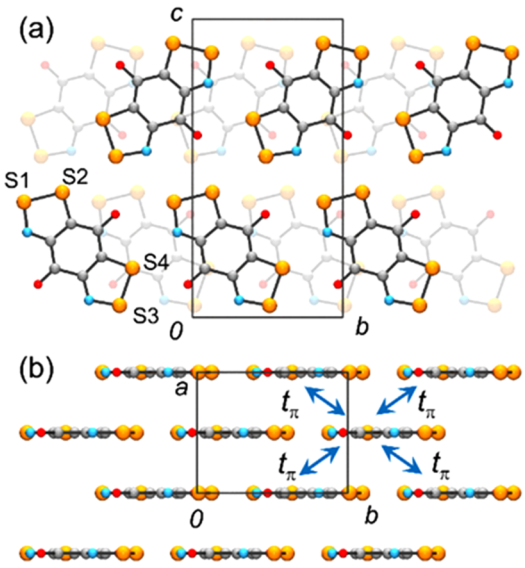

Figure 3. (a) Unit cell of **5**, showing sheet-like packing in the *bc* plane; the shaded layer is offset by *a*/2. (b) 2D brick-wall π-stacking of molecules in the *ab* plane, with four equivalent interlayer hopping interactions t_π.

As noted above, zwitterion **5** carries appeal from a solid state perspective because of its structural similarity to radical **6**; the two compounds constitute an isostructural "matched pair" in the space group $Cmc2_1$. In each case, there are four molecules in the unit cell (Figure 3), located on crystallographic planes at x = 0, 1/2, and within these coplanar layers neighboring molecules along the z-direction are related by 2-fold screw axes. Although there are small, expected differences in the internal metrics of the two compounds (Table S2), the coplanar sheet-like molecular arrays are essentially identical; the network of close (inside van der Waals separation)[13] intermolecular S···N′ and S···O′ contacts found in **5** maps perfectly onto the S···N′ and S···O′ (and S···F′) contacts found in **6** (Figure S2).[9] Adjacent layers of radicals along the x-direction are related by b-glides at x = 1/4 and 3/4, which produces a classic "brick-wall" packing pattern in the *ab* plane, with interlayer separation of *a*/2, or 3.164 (2) Å for **5** and 3.151(1) Å for **6**.[9] The number and closeness of the intermolecular contacts occasioned by this 2D architecture, in particular the four equivalent π-type hopping interactions t_π, has a profound impact on the transport properties of both compounds.

Despite the absence of unpaired spins present in radical **6**, zwitterion **5** shows remarkably high conductivity for a metal-free single component system. Variable temperature (VT) 4-probe single crystal measurements taken parallel (||) and perpendicular (⊥) to the *ab* plane (Figure 4a) indicate significant anisotropy, with enhanced performance within the brick-wall arrays, resulting

DOI: 10.1021/jacs.6b12814
J. Am. Chem. Soc. 2017, 139, 2180−2183

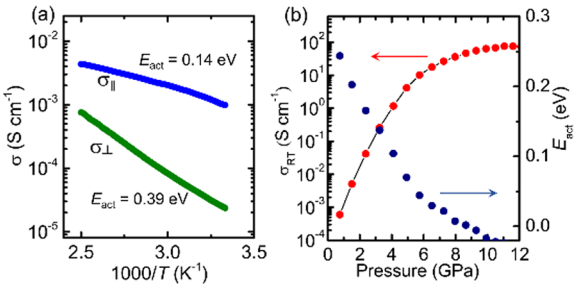

Figure 4. (a) Single crystal conductivity σ of **5** as function of temperature measured ∥ and ⊥ to the *ab* plane, with corresponding E_{act} values. (b) Pressure dependence of pressed pellet conductivity σ_{RT} and thermal activation energy E_{act} of **5**, measured using a multianvil press.

in σ_{RT} (∥) = 1.0 × 10^{-3} S cm^{-1} and E_{act} (∥) = 0.14 eV, with σ_{RT} (∥):σ_{RT} (⊥) ∼ 50:1. This behavior may be compared to that of the donor−acceptor conductor bisthiadiazolo *p*-quino-bisdithiole (BTQBT).[14] To explore the response of both σ_{RT} and E_{act} of **5** to applied pressure, we performed high pressure (HP) 4-probe conductivity measurements over the range *P* = 0−12 GPa on a pressed pellet sample using a multianvil press. The results (Figure 4b) indicate a rapid rise in σ_{RT} with increasing pressure to a non-plateau value near 10^2 S cm^{-1} at *P* = 12 GPa. At the same time, the value of E_{act} (measured over the range *T* = 25−150 °C) steadily drops, reaching zero near 8 GPa.

To explore the electronic origins of the remarkably high value of σ_{RT} for **5** observed at ambient pressure, and also its rapid pressure induced transformation to a metal, we have explored its band electronic structure as a function of pressure. As a first step, HP crystallographic studies were performed using synchrotron radiation and DAC techniques. Powder diffraction data were collected at room temperature as a function of increasing pressure up to 12 GPa, with helium as the pressure transmitting medium. The data sets so obtained were indexed and the structures solved in DASH and refined in GSAS using a molecular model derived from the ambient pressure crystal structure. In the final Rietveld refinement only the unit cell parameters were optimized. As shown in Figure 5, which illustrates variations in the unit cell dimensions of **5** as a function of pressure, there is no evidence for a structural phase change. All three axes contract uniformly, the most significant response being parallel to the *a*-axis, as found previously for **6**, an observation that reflects the relative ease of compression of the layered π-stacks.

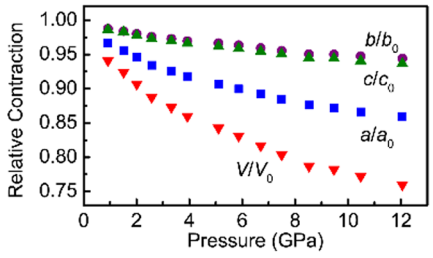

Figure 5. Contraction in unit cell dimensions of **5** with applied pressure.

Using the unit cell parameters and atomic coordinates provided by the HP structural work, we performed DFT band structure calculations using the Quantum Espresso[15] package with ultrasoft PBE pseudopotentials,[16] a plane-wave cutoff of 25 Ry and a 250 Ry integration mesh. The SCF calculations were based on crystallographic atomic coordinates and employed a 4 × 4 × 4 Monkhorst−Pack *k*-point mesh. The resulting band structure (Figure 6) can be understood in terms of the three frontier orbitals in Figure 2. In the first Brillouin zone, the valence band is composed of two crystal orbitals (COs) arising from the b_1 HOMO, whereas the conduction band comprises four COs arising from heavily hybridized (in-phase and out-of-phase) combinations of the a_2 LUMO and b_1 LUMO+1.[17]

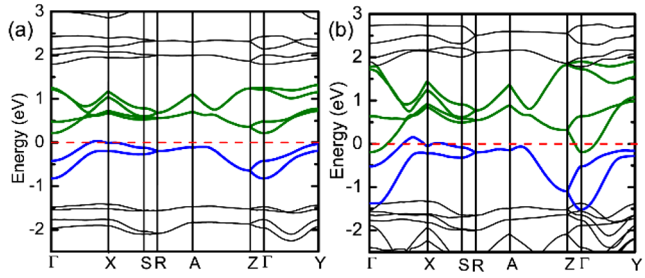

Figure 6. DFT calculated band structure of **5** at (a) 0 GPa and (b) 7.4 GPa. COs in the valence band (in blue) derive from the molecular HOMO, whereas the conduction band (in green) is composed of hybridized COs based on the LUMO and LUMO+1 (in Figure 2). The Fermi level is shown in red.

It is evident that at 0 GPa there is already significant dispersion in both the valence (0.9 eV) and conduction bands (1.0 eV), to afford an indirect band gap E_g near 0.2 eV (Figure 6a), which is significantly smaller than that calculated for BTQBT (∼1.1 eV)[18] but close to that estimated from the VT conductivity measurements (E_g ∼ 2 E_{act} (∥) = 0.28 eV). The slight discrepancy may be related to the tendency of DFT methods to underestimate correlation effects.[19] As expected, band dispersion is greatest along the reciprocal space directions Γ → X and Γ → Y, which correspond in real space to interactions within the brick-wall arrays. By comparison, interactions between neighboring walls (Γ→ Z) are small. With applied pressure, dispersion in all directions increases, including Γ → Z, as neighboring walls are compressed together. By 7.4 GPa, overall dispersion of the valence band is near 1.6 eV, whereas the width of the conduction band is over 2.0 eV. As a result, there is significant overlap of the two bands, suggestive of formation of a metallic state.

Pressure induced metallization of single component, closed shell organic (metal-free) materials by band gap closure has only rarely been observed, and pressures >30 GPa are usually required.[20] The presence of sulfur,[21] selenium[22] and tellurium[23] heteroatoms can facilitate intermolecular interactions, but even then metallic or metallike behavior requires pressures approaching or in excess of 20 GPa. In this light, the onset of a metallic state in **5** at 8 GPa by closure of the band gap without molecular deformation[24] is exceptional. The phenomenon results, we postulate, from the combination of (i) the small HOMO−LUMO gap in the molecular building block and (ii) the highly 2D solid state electronic structure afforded by its brick-wall packing pattern. Although this architecture is known to improve the performance of organic FET materials,[8] electronic interactions therein are typically cloaked by steric congestion and the actual band gap remains large. By contrast, the total absence of steric crowding in **5** allows for enhanced intrawall and (with pressure) interwall interactions, so that dispersion of the valence and conduction bands is substantial, even at ambient pressure. Given the presence of this chemical pressure, very little physical pressure is required to close the residual band gap.

DOI: 10.1021/jacs.6b12814
J. Am. Chem. Soc. 2017, 139, 2180−2183

Investigation of possible applications of **5** and related selenium-containing materials in the design of electronic, optical and thermoelectric[25] devices are in progress. Substitutional doping experiments[26] involving **5** and **6** are also being explored.

■ ASSOCIATED CONTENT

Supporting Information

The Supporting Information is available free of charge on the ACS Publications website at DOI: 10.1021/jacs.6b12814.

Experimental details and data (PDF)
Crystal data for [**5**][HOTf] (CIF)
Crystal data for **5** (CIF)
High pressure crystal data for **5** (CIF)

■ AUTHOR INFORMATION

Corresponding Author

*oakley@uwaterloo.ca

ORCID

Richard T. Oakley: 0000-0002-7185-2580

Notes

The authors declare no competing financial interest.

■ ACKNOWLEDGMENTS

We thank the NSERC of Canada and the U.S. NSF (Grant DMR 1309146) for financial aid, the NSERC for a postgraduate scholarship to S.M.W., the Government of Canada for a Tier I Canada Research Chair to J.S.T., and the Canada Foundation for Innovation for funding to R.A.S. for a 3000 ton multianvil press.

■ REFERENCES

(1) (a) Bässler, H.; Köhler, A. *Top. Curr. Chem.* **2011**, *312*, 1. (b) Coropceanu, V.; Cornil, J.; da Silva Filho, D. A.; Olivier, Y.; Silbey, R.; Brédas, J. L. *Chem. Rev.* **2007**, *107*, 926. (c) Lin, Z.; Li, Y.; Zhan, X. *Chem. Soc. Rev.* **2012**, *41*, 4245.

(2) (a) Routaboul, L.; Braunstein, P.; Xiao, J.; Zhang, Z.; Dowben, P. A.; Dalmas, G.; Da Costa, V.; Félix, O.; Decher, G.; Rosa, L. G.; Doudin, B. *J. Am. Chem. Soc.* **2012**, *134*, 8494. (b) Zheng, Y.; Wudl, F. *J. Mater. Chem. A* **2014**, *2*, 48. (c) Henson, Z. B.; Müllen, K.; Bazan, G. C. *Nat. Chem.* **2012**, *4*, 699. (d) Perepichka, D. P.; Bryce, M. R. *Angew. Chem., Int. Ed.* **2005**, *44*, 5370.

(3) (a) Constantinides, C. P.; Koutentis, P. A.; Schatz, J. *J. Am. Chem. Soc.* **2004**, *126*, 16232. (b) Langer, P.; Amiri, S.; Bodtke, A.; Saleh, N. N. R.; Weisz, K.; Görls, H.; Schreiner, P. R. *J. Org. Chem.* **2008**, *73*, 5048. (c) Amiri, S.; Schreiner, P. R. *J. Phys. Chem. A* **2009**, *113*, 11750. (e) Zhang, G. B.; Li, S. H.; Jiang, J. S. *J. Phys. Chem. A* **2003**, *107*, 5573.

(4) (a) Hutchison, K.; Srdanov, G.; Hicks, R.; Yu, H.; Wudl, F.; Strassner, T.; Nendel, M.; Houk, K. N. *J. Am. Chem. Soc.* **1998**, *120*, 2989. (b) Wudl, F.; Koutentis, P. A.; Weitz, A.; Ma, B.; Strassner, T.; Houk, K. N.; Khan, S. I. *Pure Appl. Chem.* **1999**, *71*, 295. (c) Gampe, D. M.; Kaufmann, M.; Jakobi, D.; Sachse, T.; Presselt, M.; Beckert, R.; Görls, H. *Chem. - Eur. J.* **2015**, *21*, 7571. (d) Constantinides, C. P.; Ioannou, T. A.; Koutentis, P. A. *Polyhedron* **2013**, *64*, 172. (e) Constantinides, C. P.; Zissimou, G. A.; Berezin, A. A.; Ioannou, T. A.; Manoli, M.; Tsokkou, D.; Theodorou, E.; Hayes, S. C.; Koutentis, P. A. *Org. Lett.* **2015**, *17*, 4026.

(5) (a) Leitch, A. A.; Oakley, R. T.; Reed, R. W.; Thompson, L. K. *Inorg. Chem.* **2007**, *46*, 6261. (b) Beer, L.; Cordes, A. W.; Oakley, R. T.; Mingie, J. R.; Preuss, K. E.; Taylor, N. J. *J. Am. Chem. Soc.* **2000**, *122*, 7602.

(6) In thin films of quinonemonoimines, semimetallic behavior has been observed. See, for example: (a) Rosa, L. G.; Velev, J.; Zhang, Z.; Alvira, J.; Vega, O.; Diaz, G.; Routaboul, L.; Braunstein, P.; Doudin, B.; Losovyj, Y. B.; Dowben, P. A. *Phys. Status Solidi B* **2012**, *249*, 1571. (b) Yuan, M.; Tanabe, I.; Bernard-Schaaf, J. M.; Shi, Q. Y.; Schlegel, V.; Schurhammer, R.; Dowben, P. A.; Doudin, B.; Routaboul, L.; Braunstein, P. *New J. Chem.* **2016**, *40*, 5782.

(7) Winter, S. M.; Roberts, R. J.; Mailman, A.; Cvrkalj, K.; Assoud, A.; Oakley, R. T. *Chem. Commun.* **2010**, *46*, 4496.

(8) (a) Payne, M. M.; Parkin, S. R.; Anthony, J. E.; Kuo, C.-C.; Jackson, T. N. *J. Am. Chem. Soc.* **2005**, *127*, 4986. (b) Dong, H.; Wang, C.; Hu, W. *Chem. Commun.* **2010**, *46*, 5211. (c) He, T.; Stolte, M.; Burschka, C.; Hansen, N. H.; Musiol, T.; Kälblein, D.; Pflaum, J.; Tao, X.; Brill, J.; Würthner, F. *Nat. Commun.* **2015**, *6*, 5954. (d) Illig, S.; Eggeman, A. S.; Troisi, A.; Jiang, L.; Warwick, C.; Nikolka, M.; Schweicher, G.; Yeates, S. G.; Geerts, H. Y.; Anthony, J. E.; Sirringhaus, H. *Nat. Commun.* **2016**, *7*, 10736.

(9) Mailman, A.; Winter, S. M.; Yu, X.; Robertson, C. M.; Yong, W.; Tse, J. S.; Secco, R. A.; Liu, Z.; Dube, P. A.; Howard, J. A. K.; Oakley, R. T. *J. Am. Chem. Soc.* **2012**, *134*, 9886.

(10) Tian, D.; Winter, S. M.; Mailman, A.; Wong, J. W. L.; Yong, W.; Yamaguchi, H.; Jia, Y.; Tse, J. S.; Desgreniers, S.; Secco, R. A.; Julian, S. R.; Jin, C.; Mito, M.; Ohishi, Y.; Oakley, R. T. *J. Am. Chem. Soc.* **2015**, *137*, 14136.

(11) (a) Nissen, F.; Detert, H. *Eur. J. Org. Chem.* **2011**, *2011*, 2845. (b) Zemplen, G.; Schawartz, J. *Acta. Chim. Sci. Hungaricae* **1953**, *3*, 487.

(12) A similarly small a_N value (0.101 mT) has been found in the isomeric benzoquinone-bridged bis-1,3,2-dithiazolylium radical cation. See: Decken, A.; Mailman, A.; Passmore, J. *Chem. Commun.* **2009**, 6077.

(13) (a) Bondi, A. *J. Phys. Chem.* **1964**, *68*, 441. (b) Dance, I. *New J. Chem.* **2003**, *27*, 22.

(14) For BTQBT $\sigma_{RT} \sim 10^{-3}$ S cm^{-1} and $E_{act} = 0.21$ eV, see: Inokuchi, H.; Imaeda, K. *Acta Phys. Pol., A* **1995**, *88*, 1161.

(15) Giannozzi, P.; Baroni, S.; Bonini, N.; Calandra, M.; Car, R.; Cavazzoni, C.; Ceresoli, D.; Chiarotti, G. L.; Cococcioni, M.; Dabo, I.; Dal Corso, A.; Fabris, S.; Fratesi, G.; de Gironcoli, S.; Gebauer, R.; Gerstmann, U.; Gougoussis, C.; Kokalj, A.; Lazzeri, M.; Martin-Samos, L.; Marzari, N.; Mauri, F.; Mazzarello, R.; Paolini, S.; Pasquarello, A.; Paulatto, L.; Sbraccia, C.; Scandolo, S.; Sclauzero, G.; Seitsonen, A. P.; Smogunov, A.; Umari, P.; Wentzcovitch, R. M. *J. Phys.: Condens. Matter* **2009**, *21*, 395502.

(16) (a) Perdew, J. P.; Burke, K.; Ernzerhof, M. *Phys. Rev. Lett.* **1996**, *77*, 3865. (b) Perdew, J. P.; Burke, K.; Ernzerhof, M. *Phys. Rev. Lett.* **1997**, *78*, 1396.

(17) Winter, S. M.; Mailman, A.; Oakley, R. T.; Thirunavukkuarasu, K.; Hill, S.; Graf, D. E.; Tozer, S. W.; Tse, J. S.; Mito, M.; Yamaguchi, H. *Phys. Rev. B: Condens. Matter Mater. Phys.* **2014**, *89*, 214403.

(18) Huang, J.; Kertesz, M. *J. Phys. Chem. B* **2005**, *109*, 12891.

(19) Hybertsen, M. S.; Louie, S. G. *Phys. Rev. B: Condens. Matter Mater. Phys.* **1986**, *34*, 5390.

(20) (a) Aust, R. B.; Bentley, W. H.; Drickamer, H. G. *J. Chem. Phys.* **1964**, *41*, 1856. (b) Saito, G.; Yoshida, Y. *Bull. Chem. Soc. Jpn.* **2007**, *80*, 1.

(21) Cui, H.; Brooks, J. S.; Kobayashi, A.; Kobayashi, H. *J. Am. Chem. Soc.* **2009**, *131*, 6358.

(22) (a) Shirotani, I.; Kamura, Y.; Inokuchi, H.; Hirooka, T. *Chem. Phys. Lett.* **1976**, *40*, 257. (b) Onodera, A.; Shirotani, I.; Inokuchi, H.; Kawai, N. *Chem. Phys. Lett.* **1974**, *25*, 296.

(23) (a) Cui, H.; Okano, Y.; Zhou, B.; Kobayashi, A.; Kobayashi, H. *J. Am. Chem. Soc.* **2008**, *130*, 3738. (b) Tulip, P. R.; Bates, S. P. *J. Phys. Chem. C* **2009**, *113*, 19310.

(24) Tse, J. S.; Leitch, A. A.; Yu, X.; Bao, X.; Zhang, S.; Liu, Q.; Jin, C.; Secco, R. A.; Desgreniers, S.; Ohishi, Y.; Oakley, R. T. *J. Am. Chem. Soc.* **2010**, *132*, 4876.

(25) (a) Shi, W.; Chen, J.; Xi, J.; Wang, D.; Shuai, Z. *Chem. Mater.* **2014**, *26*, 2669. (b) Di, C.; Xu, W.; Zhu, D. *Natl. Sci. Rev.* **2016**, *3*, 269.

(26) (a) Mebrouk, K.; Kaddour, W.; Auban-Senzier, P.; Pasquier, C.; Jeannin, O.; Camerel, F.; Fourmigué, M. *Inorg. Chem.* **2015**, *54*, 7454. (b) Pal, S. K.; Bag, P.; Itkis, M. E.; Tham, F. S.; Haddon, R. C. *J. Am. Chem. Soc.* **2014**, *136*, 14738. (b) Bag, P.; Itkis, M. E.; Stekovic, D.; Pal, S. K.; Tham, F. S.; Haddon, R. C. *J. Am. Chem. Soc.* **2015**, *137*, 10000.

DOI: 10.1021/jacs.6b12814
J. Am. Chem. Soc. 2017, 139, 2180−2183